JOURNAL OF Applied Polymer SCIENCE

Interior Synthesizing of ZnO Nanoflakes Inside Nylon-6 Electrospun Nanofibers

Gopal Panthi,[1] Nasser A. M. Barakat,[2,3] Salem S. Al-Deyab,[4] Mohamed El-Newehy,[4,5] Dipendra Raj Pandeya,[6] Hak Yong Kim[2]

[1]Department of Bionano System Engineering, College of Engineering, Chonbuk National University, Jeonju 561-756, Republic of Korea
[2]Organic Materials and Fiber Engineering Department, Chonbuk National University, Jeonju 561-756, Republic of Korea
[3]Chemical Engineering Department, Minia University, El-Minia, Egypt
[4]Department of Chemistry, College of Science, King Saud University, Riyadh 11451, Saudi Arabia
[5]Faculty of Science, Department of Chemistry, Tanta University, Tanta 31527, Egypt
[6]Department of Microbiology and Immunology, Institute of Medical Science, Chonbuk National University Medical School, Jeonju 561-756, Republic of Korea
Correspondence to: N. A. M. Barakat (E-mail: nasser@jbnu.ac.kr) or H. Y. Kim (E-mail: khy@jbnu.ac.kr)

ABSTRACT: Doping of the polymeric electrospun nanofibers by metal oxides nanoparticles is usually performed by electrospinning of a colloidal solution containing the metal oxide nanoparticles. Besides the economical aspects, electrospinning of colloids is not efficient compared with spinning of sol–gels, moreover well attachment of the solid nanoparticles is not guaranteed. In this study, reduction of zinc acetate could be performed inside the nylon-6 electrospun nanofibers; so polymeric nanofibers embedding ZnO nanoflakes were obtained. Typically, zinc acetate/nylon-6 electrospun nanofibers were treated hydrothermally at 150°C for 1 h. Besides the utilized characterization techniques, PL study affirmed formation of ZnO. The produced nanofibers showed a good antibacterial activity which improves with increasing ZnO content. Overall, the present study opens new avenue to synthesize hybrid nanofibers by a facile procedure. © 2012 Wiley Periodicals, Inc. J. Appl. Polym. Sci. 000: 000–000, 2012

KEYWORDS: hybrid nanofibers; nanocomposites; ZnO; nylon-6; electrospinning; antibacterial

Received 29 November 2011; accepted 5 March 2012; published online
DOI: 10.1002/app.37639

INTRODUCTION

Nanofibers are an exciting class of material used for several value added applications such as medical, filtration, barrier, wipes, personal care, composite, garments, insulation, and energy storage.[1,2] The electrospinning technique has been proven to be versatile and effective method for manufacturing micro to nano scale fibers.[3] Inorganic nanostructures in general reveal fantastic characteristics; however, handling is the main constrain standing against wide applications because usually the final product is in a powdery form. Therefore, hybrid nanofibers are an interesting remedy for the problem as the metal oxide NPs can be supported in an electrospun mat which can be easily handled. Usually, the metal oxides as ceramic materials are not soluble in most of the conventional solvents, accordingly electrospinning of metal oxide NPs/polymer colloids was carried out in most of the reported studies to produce metal oxide-doped polymeric nanofibers.[4,5] To incorporate the metal oxide NPs inside polymeric nanofibers, the size of the utilized NPs should be very small which creates financial problem in case of large scale production. Moreover, electrospinning of the prepared NPs/polymer colloid has low efficiency compared to sol–gels which adds another dilemma to that strategy. Accordingly, seeking about another methodology to prepare the hybrid nanofibers from a sol–gel is an interesting target. Recently, Ye et al.[6] introduced ZnO-doped cellulose nanofibers using the electrospinning and solvothermal techniques. In that study, a sol–gel consisting of zinc acetate (ZnAc) and cellulose was electrospun, and then NaOH solution was used to decompose zinc acetate into zinc oxide. To avoid utilizing the alkaline solution which might affect the mechanical properties of the polymer, we report facile and feasible route to synthesize nylon-6 mats containing ZnO nanoparticles/nanoflakes inside the polymeric nanofibers via combined electrospinning and hydrothermal processes. The formed nylon-6/ZnO hybrid mats showed good

© 2012 Wiley Periodicals, Inc.

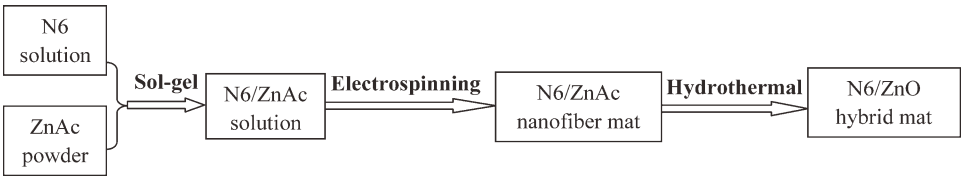

Figure 1. Synthesis sketch of nylon-6/ZnO hybrid mat.

antibacterial activity towards the gram negative bacteria (*Escherichia Coli*) in the day light condition without using UV-radiation. In other words, besides overcoming the handling problem, incorporation of ZnO inside the polymeric nanofibers did not affect the known antibacterial activity of ZnO.[7,8]

EXPERIMENTAL PROCEDURE

Hybrid Nanofibers Preparation

First, 22 wt % nylon-6 (N6, KN20 grade, Kolon, Korea) solution was prepared by dissolving the polymer granules in a formic acid/acetic acid (weight ratio of 4:1) mixed solvent. Sol–gels with different zinc acetate [ZnAc, $Zn(CH_3COO)_2{\cdot}2H_2O$, Showa, Japan] contents were prepared by addition of ZnAc powder to the polymer solution, namely the utilized solutions were having 5, 10, and 15 wt % ZnAc (based on nylon-6 solution). The final solutions were electrospun at 22 kV, the distance between the collector and the tip of the syringe was fixed to be 16 cm. Thus obtained N6/ZnAc electrospun mats were vacuously dried at 50°C for 24 h. In a typical hydrothermal process, 1.076 g of Bis-(hexamethylene)-triamine (Bis-HEA, Sigma-Aldrich) was dissolved in 50 mL distilled water, then 500 mg from the hybrid electrospun mats were added to the solution. Subsequently, the resulting mixtures were transferred into a Teflon lined stainless steel autoclave and kept at different temperatures and times. Finally, the resultant mats were drawn from the autoclave, washed several times by distilled water, and dried at 50°C for 12 h. The mats obtained from 5, 10, and 15 wt % ZnAc were named as m1, m2, and m3, respectively. The proposed procedure is schematically summarized in Figure 1.

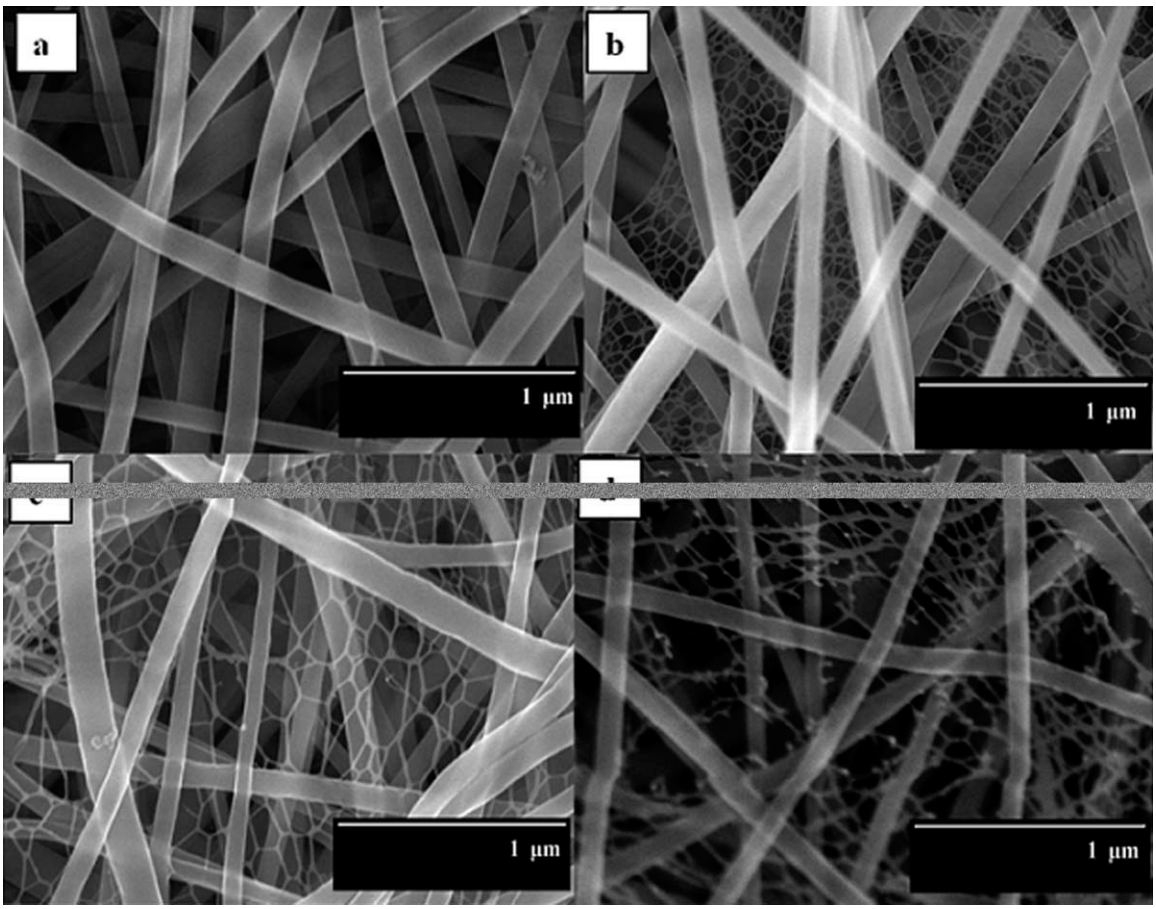

Figure 2. FESEM images of pristine nylon-6 (a) and nylon-6/ZnAc mats before hydrothermal process (b, c, and d panels represent electrospun mats containing 5, 10, and 15 wt % ZnAc, respectively).

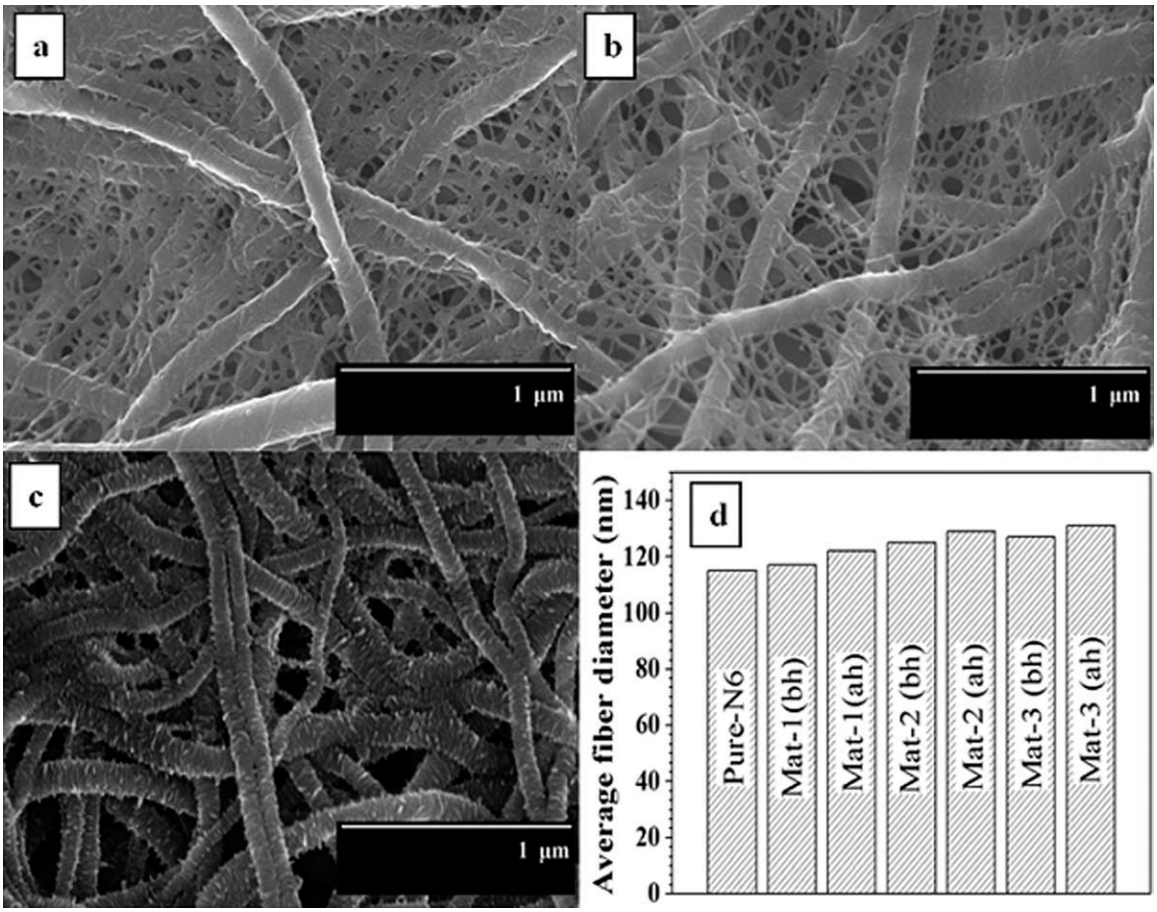

Figure 3. FESEM images of nylon-6/ZnAc mats after the hydrothermal process (a, b, and c represent samples containing 5, 10, and 15 wt %, ZnAc, respectively). Panel d represents the average diameters (bh, before hydrothermal; ah, after hydrothermal). The hydrothermal process was carried out at 150°C for 1 h.

Antibacterial Test

The antibacterial properties of the N6/ZnO hybrid mats were quantitatively evaluated using a gram-negative bacterium (*E. coli*) ATCC 52922 as a model organism. The bacterial inoculums were prepared in Triptic Soy-agar broth at 37°C for 12 h. The hybrid mats of the same diameter were cut and placed at the bottom of the Petri dish, and the *E. coli* suspension was placed over the mats and incubated at 37°C for 12 h. The cell concentration was determined by a viable count method on Triptic Soy Agar plates after 10^{-7} dilution of the culture in Triptic Soy Broth; 100 μL solutions are taken from the 10^{-7} dilution and spread on the Triptic Soy Agar plates. All the plates were incubated at 37°C for 12 h before enumeration.

Characterization

The surface morphology of nanofibers was studied by using field-emission scanning electron microscopy (FE-SEM, S-7400, Hitachi, Japan). Information about the phase and crystallinity of different mats (before and after hydrothermal process) were obtained by using a Rigaku X-ray diffractometer (XRD, Rigaku, Japan) with Cu Kα (λ = 1.540 Å) radiation over Bragg angle ranging from 10° to70°. High resolution images of nanofibers

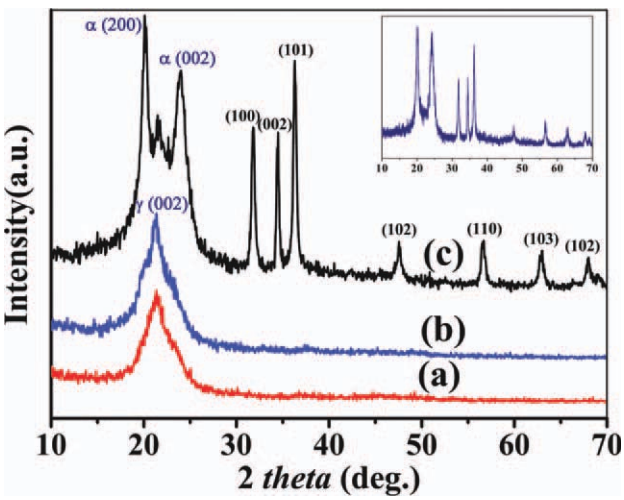

Figure 4. XRD patterns of pristine nylon-6 (a), and ZnAc-containing nylon-6 nanofibers (sample m2) before (b), and after the hydrothermal treatment (c). The inset represents XRD results for sample m3. The hydrothermal process was carried out at 150°C for 1 h. [Color figure can be viewed in the online issue, which is available at wileyonlinelibrary.com.]

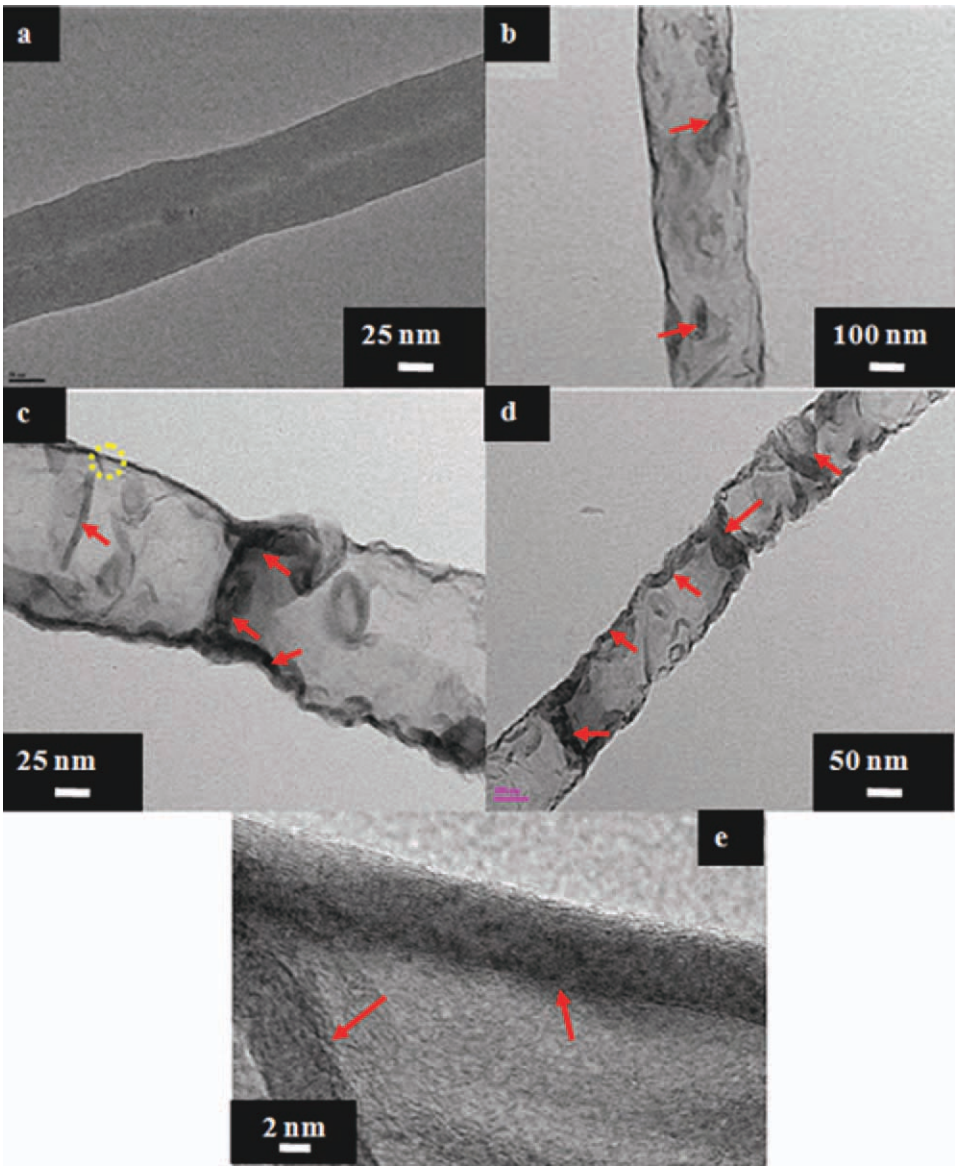

Figure 5. TEM images for nylon-6/ZnAc electrospun nanofibers before (a, sample m1) and after the hydrothermal process; (b, sample m1; c, sample m2; and d, sample m3), the red arrows point to the crystalline ZnO nanoflakes. Panel e represents the HR TEM image for the marked area in image c. The hydrothermal process was carried out at 150°C for 1 h. [Color figure can be viewed in the online issue, which is available at wileyonlinelibrary.com.]

containing ZnO nanoparticles of nanoflakes were obtained via transmission electron microscopy (TEM, JEM-2010, JEOL, Japan) operating at 200 kV. Photoluminescence (PL) spectroscopy analysis was carried out at room temperature using a laser with 325 nm wave length as the stimulating source.

RESULT AND DISCUSSION

The electrospinning technique involves the use of a high voltage to charge the surface of a polymer solution droplet and thus to induce the ejection of a liquid jet through a spinneret. Because of bending instability, the jet is subsequently stretched by many times to form continuous, ultrathin fibers. Consequently, the electrospinning is widely used for production of many polymeric nanofibers. Figure 2 displays the FE-SEM images of pristine [Figure 2(a)] and ZnAc-contained (5, 10, and 15 wt %, Figure 2(b–d), respectively) nylon-6 electrospun mats. As shown in the figure, spider-net was created among the main nanofibers due to salt addition. Actually, formation of small nanofibers in the form of spider net among the main polymer nanofibers upon salt addition was fully studied in our previous work.[9] Briefly, in that study, it was concluded that addition of a salt does have tendency to ionize in the polymer solution leads to form a spider-net like structure among the main electrospun nanofibers. Figure 3 represents the FE SEM images of samples m1, m2, and m3 mats obtained after the proposed hydrothermal process which was carried out at 150°C for 1 h [Figure 3(a–c), respectively]. Moreover, the average fiber diameter of each mat has been estimated, the results are demonstrated in Figure 3(d). As shown in the Figure 3(a, b), the spider-net

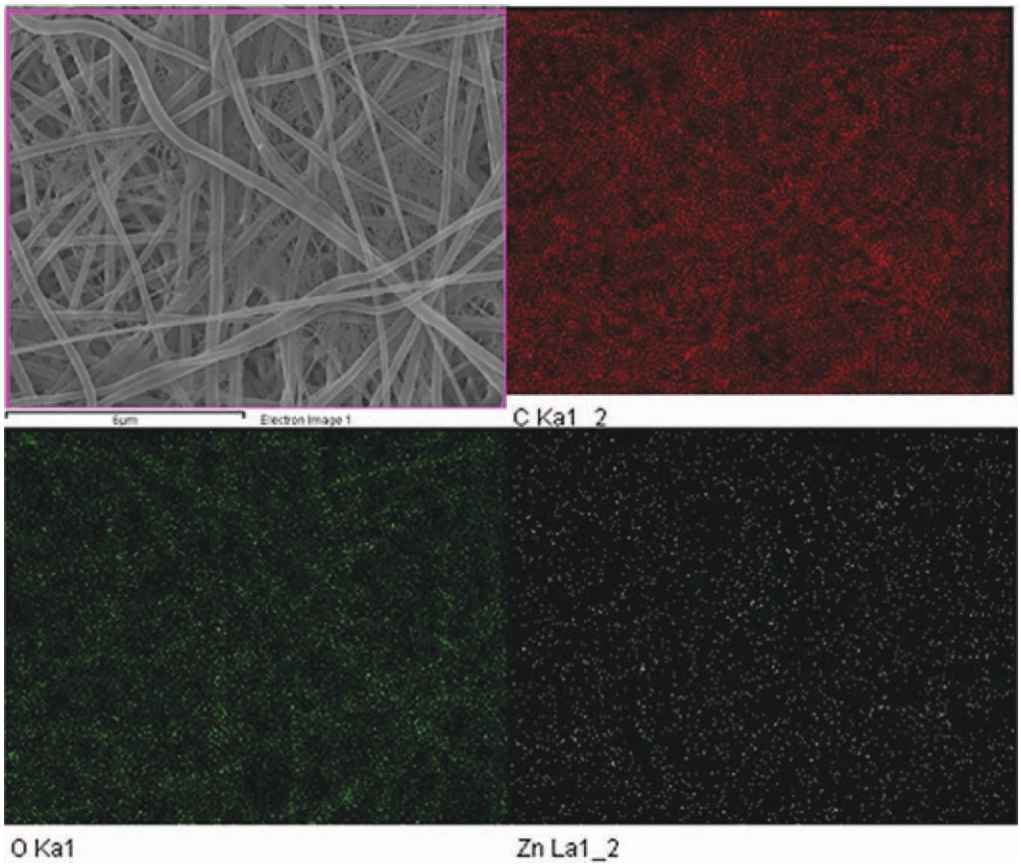

Figure 6. Elemental mapping analysis for sample m2 after the hydrothermal process. The hydrothermal process was carried out at 150°C for 1 h. [Color figure can be viewed in the online issue, which is available at wileyonlinelibrary.com.]

became denser after the hydrothermal process due to the high pressure atmosphere inside the reactor. The spider-net disappeared at high concentration of ZnAc [Figure 3(c)]. Addition of ZnAc to nylon-6 led to a slight increase in the average diameter [Figure 3(b)], the average diameter of the nanofibers was found to be 115, 117, 125, and 127 nm for the mats containing 0, 5, 10, and 15 wt % ZnAc, respectively. This increase in the average fiber diameter can be explicated as the effect of ZnAc.[10] Similarly, the average fiber diameter of m1, m2, and m3 mats was also found to be 122, 129, and 131 nm, respectively. For the same formulation, a slight increase can be observed due to the hydrothermal treatment. The average fiber diameters were estimated by using Photoshop computer software, in every image the diameters of at least 100 nanofibers were estimated and then the average value was determined.

Figure 4 represents the XRD patterns of pure and ZnAc-containing nylon-6 electrospun mat before and after hydrothermal treatment process at 150°C for 1 h. A broad non-crystalline peak at 2θ of 21.5° was observed for the pristine and ZnAc/nylon-6 formulations which represents γ nylon-6. The diffraction peaks at 2θ of 31.63°, 34.48°, 47.53°, 56.47°, 62.78°, 67.92° corresponding to the crystal planes of (100), (002), (101), (102), (110), (103), and (112) indicate the presence of ZnO in the nanofibers (JCPDS 36-1451). The introduced spectra in this figure represent the sample containing 10 wt % zinc acetate (i.e., sample m2). The inset demonstrates the results obtained when the ZnAc content was 15 wt % (i.e., sample m3), as shown in this figure the peaks representing ZnO are more sharp and have higher intensities. This observation indicates more crystalline ZnO in the treated electrospun mat in case of m3 sample. Therefore, one can say that increase the utilized amount of ZnAc in the electrospun mat leads to enhance ZnO content

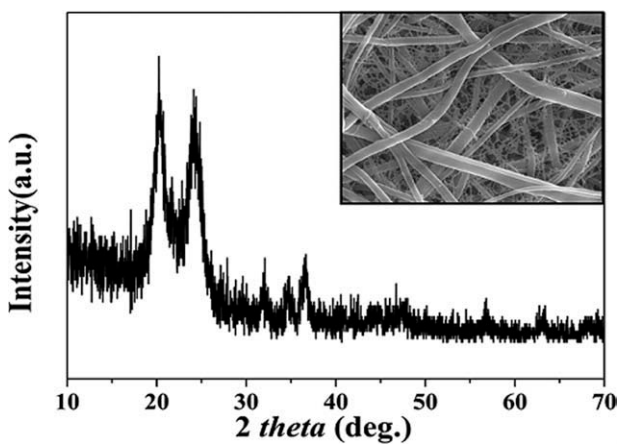

Figure 7. XRD pattern for the sample m2 after hydrothermal treatment at 125°C for 1 h. The inset shows the corresponding FE SEM image.

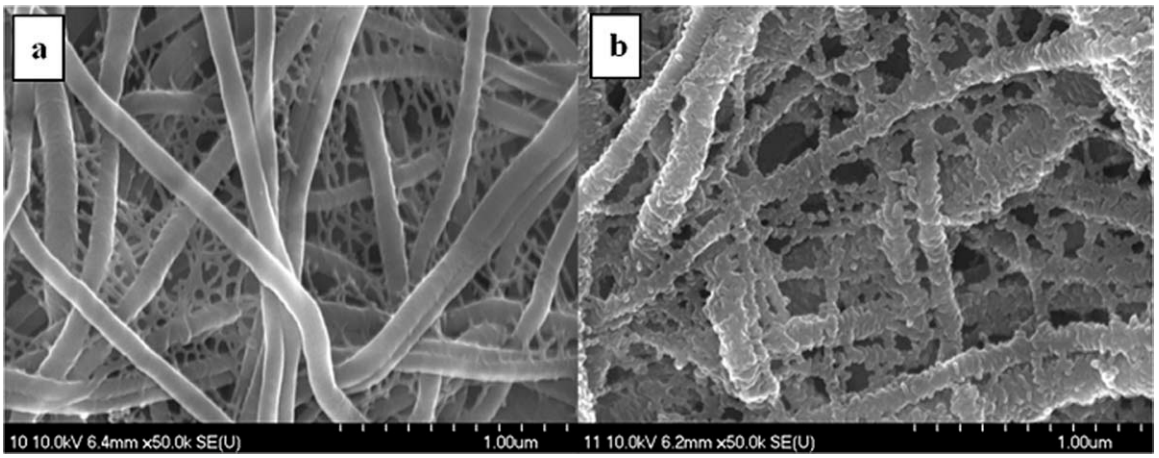

Figure 8. The obtained mat after hydrothermal treatment of m2 sample at 150°C for 30 min (a) and 90 min (b).

after the hydrothermal treatment process. Moreover, it can be said that ZnO exists in the main nanofibers rather than in the spider net counterpart as m3 sample does not contain spider net [Figure 3(c)]. This finding is interesting as the proposed hydrothermal process could reduce the ZnAc to ZnO, which was carried out inside the polymer nanofibers. It is noteworthy mentioning that, the proposed hydrothermal process could convert nylon-6 from γ to α form, the later being thermodynamically the most stable. Interestingly, increase ZnAc content causes to complete transformation of nylon-6 from γ to α form as shown in the inset.

The direct evidence of formation of ZnO inside the nylon-6 fibers was further given by TEM images (Figure 5). As shown in Figure 5(a), which represents TEM image of sample m1 before the proposed hydrothermal process, there is no crystalline parts can be observed. It is clearly seen that the crystalline ZnO nanoflake-like structures are formed inside the nylon-6 fibers due to the hydrothermal treatment process in all formulations [Figure 5(b–d)]. From Figure 5(d) it is shown that ZnO crystals are formed in large quantities in m3 mat but it is formed in small quantities in m1 and m2 mats [Figure 5(b, c), respectively]. This may be due to the low content of ZnAc in m1 and m2 mats. This finding supports the XRD results. The crystalline structure of ZnO was further confirmed by high resolution TEM image [Figure (5e)]. Figure 6 represents the elemental mapping of the treated nylon-6/ZnAc (sample m2), as shown in the figure carbon and oxygen have high density as they are incorporated in the polymer chain, however zinc has a relatively low density. Also, from the elemental mapping, one can suggest good distribution of ZnO inside the treated nanofibers.

To properly investigate the influence of the temperature and time as important process parameters, the hydrothermal treatment process was carried out at 125 and 175°C. Figure 7 displays the XRD results for the m2 sample obtained at temperature of 125°C and residing time of 1 h. As shown in the figure, weak ZnO peaks can be observed which suggests low ZnO content. The inset represents the corresponding FE SEM image of the obtained nanofiber mat, as shown little change in the morphology can be observed. Increasing the hydrothermal temperature to 175°C resulted in complete disappearing of the polymer nanofibers, only small pasty powder was obtained. Accordingly, performing the hydrothermal process at 150°C is highly recommended. Concerning the treatment time, Figure 8(a) and (b) represent the FE SEM images for the sample m2 after hydrothermal treatment at 30 and 90 min, respectively. As shown in Figure 8(a), short treatment time looks insufficient to convert ZnAc to ZnO as there is not distinct change in the morphology. In other words, the nanofibers' surfaces turn to be rough due to ZnO incorporation as can be concluded from the previous images, so Figure 8(a) reveals low ZnO content as the surfaces are smooth and almost there is no change in the spider net morphology. The XRD results showed very weak peaks (data not shown). However, as shown in Figure 8(b), as expected, long treatment time have good impact of ZnO formation as the surface of the nanofibers became rough due to ZnO formation.

It is commonly known that the room temperature PL spectra for ZnO usually show three major peaks: a UV near-band-edge emission peak around 380 nm, a green emission peak around

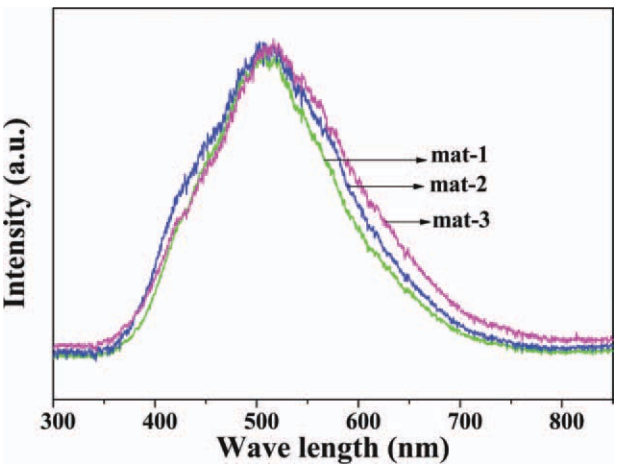

Figure 9. PL spectra of m1, m2, and m3 mats. [Color figure can be viewed in the online issue, which is available at wileyonlinelibrary.com.]

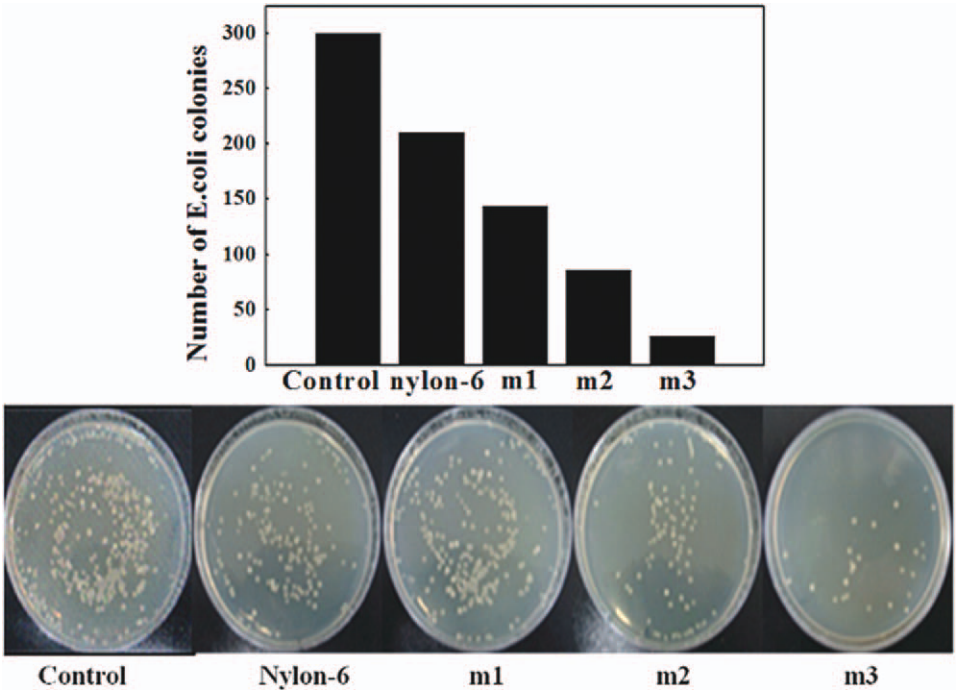

Figure 10. Number of *E. coli* colonies grown on LB agar plates after treatment. [Color figure can be viewed in the online issue, which is available at wileyonlinelibrary.com.]

520 nm, and a yellow–orange emission peak around 600 nm. The 380 nm peak is attributed to the exciton recombination process, whereas the green and orange are attributed to the intrinsic defect of ZnO.[11–13] In this study, the peaks obtained around 520 nm were attributed to deep level intrinsic defect in ZnO crystals such as vacancies and interstitials of zinc and oxygen (Figure 9).

Figure 10 shows the antibacterial activity on the surface of different composite mats against *E. coli* in the day light. The result showed that the m3 mat has the lowest survivability of bacteria than that of m2 and m3 mats. It showed that the pristine nylon-6 mat did not show remarkable antibacterial activity. The suggested two possible mechanisms for the antibacterial activity of zinc oxide nanoparticles towards *E. coli* are: (i) Formation of increased levels of reactive oxygen species (ROS) mainly hydroxyl radical and singlet oxygen which damage the bacterial cell wall.[14–16] (ii) Deposition of nanoparticles on the surface of bacteria or accumulation of the nanoparticles either in the cytoplasm or in the periplasm region causing disruption of cellular function and disorganization of membranes.[17] In the present study, the second hypothesis is not valid as ZnO is incorporated inside the nanofibers.

CONCLUSION

Hydrothermal treatment of zinc acetate/nylon-6 electrospun nanofibers in presence of suitable reducing agent can lead to produce of nylon-6 nanofibers embedding ZnO flakes. This strategy might be invoked to produce metal oxide-doped polymeric nanofibers rather than electrospinning of colloidal solution; the conventional complicated methodology. Interestingly, ZnO doping of the nylon-6 nanofibers did not affect the antibacterial activity and PL characteristic of the ZnO.

ACKNOWLEDGMENTS

This research was supported by NPST program by King Saud University project number 11-ENE1721-02. The authors thank Mr. T. S. Bae and J. C. Lim, KBSI, Jeonju branch, and Mr. Jong- Gyun Kang, Centre for University Research Facility, for taking high-quality FESEM and TEM images, respectively.

REFERENCES

1. Ramakrishna, S.; Fujihara, K.; Toe, W. E.; Yong, T.; Ma, Z. W.; Ramaseahan, R. *Mater. Today* **2006,** *9*, 40.
2. Wenk, G. E.; Carr, M. E.; Simpson, D. G.; Bowlin, G. L. *Nano Lett.* **2003,** *3*, 213.
3. Wang, X. Y.; Drew, C.; Lee, S. H.; Senecal, K. J.; Kumar, J.; Samuelson, L. A. *Nano Lett.* **2002,** *2*, 1273.
4. Im, J. S.; Kim, I. M.; Lee, Y. S. *Mater. Lett.* **2008,** *64*, 3652.
5. Pant, H. R.; Bajgai, M. P.; Nam, K. T.; Seo, Y. A.; Pandeya, D. R.; Hong, S. T.; Kim, H. Y. *J. Hazard. Mater.* **2010,** *185*, 124.
6. Ye, S.; Zhang, D.; Liu, H.; Zhou, J. *J. Appl. Polym. Sci.* **2011,** *121*, 1757.
7. Brayner, R.; Ferrari-Iliou, R.; Brivois, N.; Djediat, S.; Benedetti, M. F.; Fievet, F. *Nano Lett.* **2006,** *6*, 866.
8. Jones, N.; Ray, B.; Koodali, R.; Manna, A. C. *FEMS Microbiol. Lett.* **2008,** *279*, 71.
9. Barakat, N.A. M. ;Kanjwal, A. M.; Sheikh, F. A. ;Kim, H. Y. *Polymer* **2009,** *50*, 4389.

10. Horzum, N.; Tascioglu, D.; Okur, S.; Demir, M. M. *Tantala* **2011,** *85*, 1105.
11. Xia, T.; Kovochich, M.; Adler, L. M.; Gilbert, B.; Shi, H.; Yeh, J. I.; Zink, J. I.; Nel, A. E. *ACS Nano.* **2008,** *2*, 2121.
12. Yang, H.; Liu, C.; Yang, D.; Zhang, H.; Xi, Z. J. *Appl. Toxicol.* **2009,** *29*, 69.
13. Bery, V.; Gole, A.; Kundu, S.; Murphy, C. J.; Saraf, R. F. *J. Am. Chem. Soc.* **2005,** *127*, 17600.
14. Zhang, L.; Jiang, Y.; Ding, Y.; Povey, M.; York, D. J. *Nanopart. Res.* **2007,** *9*, 479.
15. Li, D.; Leung, Y. H.; Djurisic, A. B.; Liu, Z. T.; Xie, M. H.; Shi, S. L.; Xu, S. J.; Chan, W. K. *Appl. Phys. Lett.* **2004,** *85*, 1601.
16. Lyu, S. C.; Zhang, Y.; Ruh, Y. H.; Lee, H. J.; Shim, H. W.; Suh, E. K.; Lee, C. *J. Chem. Phys. Lett.* **2002,** *363*, 134.
17. Studenikin, S. A.; Golego, N.; Cocivera, M. J. *Appl. Phys.* **1998,** *84*, 2287.